New Phytologist

Forum

Viewpoint

Shining a new light on the classical concepts of carbon-isotope dendrochronology

Summary

Retrospective information about plant ecophysiology and the climate system are key inputs in Earth system and vegetation models. Dendrochronology provides such information with large spatiotemporal coverage, and carbon-isotope analysis across tree-ring series is among the most advanced dendrochronological tools. For the past 70 years, this analysis was performed on whole molecules and, to this day, ^{13}C discrimination during carbon assimilation is invoked to explain isotope variation and associated climate signals. However, recently it was reported that tree-ring glucose exhibits multiple isotope signals at the intramolecular level (see Wieloch *et al*., 2025). Here, I estimated the signals' contribution to whole-molecule isotope variation and found that downstream processes in leaf and stem metabolism each introduce more variation than carbon assimilation. Moreover, downstream processes introduce most of the climate information. These findings are inconsistent with the classical concepts/practices of carbon-isotope dendrochronology. More importantly, intramolecular tree-ring isotope analysis promises novel insights into forest metabolism and the climate of the past.

Introduction

Tree rings are natural archives containing encoded information about plant metabolic processes, their environmental dependences, and the climate of the past. This information is (to a large extent) inaccessible to manipulation and monitoring experiments, and dendrochronologists strive to decipher it to contribute to a better understanding of the climate system, plant functioning, and biogeochemical cycles. Stable carbon-isotope (^{12}C, ^{13}C) analysis across tree-ring series is among the most advanced dendrochronological tools available today. This tool has (*inter alia*) been used to reconstruct leaf intrinsic water-use efficiency (CO_2 uptake relative to H_2O loss, *iWUE*), air temperature, solar radiation, relative humidity, precipitation, and drought over past centuries at numerous locations world-wide (Cernusak & Ubierna, 2022; Gagen *et al*., 2022).

Seventy years ago, tree-ring ^{13}C : ^{12}C ratios were measured for the first time (Craig, 1953, 1954). While early studies analysed whole-wood samples, most recent studies analyse cellulose, a glucose polymer extracted from tree rings to preclude error due to variation in wood composition (Helle *et al*., 2022). Note, arguments given below apply to glucose and cellulose but not necessarily to wood. Tree-ring cellulose ^{13}C : ^{12}C data are commonly expressed in terms of ^{13}C discrimination, Δ_{trc}, denoting carbon-isotope changes caused by physiological processes (Farquhar & Richards, 1984). Current data interpretation invokes a simplified mechanistic model of ^{13}C discrimination accounting for two processes: CO_2 diffusion from ambient air into leaf intercellular air spaces, and carbon assimilation by rubisco (Farquhar *et al*., 1982; McCarroll & Loader, 2004; Cernusak & Ubierna, 2022), combinedly termed diffusion-rubisco (DR) discrimination (Wieloch *et al*., 2018).

Variation in DR discrimination depends on the ratio of intercellular-to-ambient CO_2 concentration (Farquhar *et al*., 1982; Evans *et al*., 1986; Voelker *et al*., 2016). Intercellular CO_2 concentration, in turn, varies with the rate of CO_2 supply through leaf stomata and the rate of CO_2 assimilatory demand. As stomata respond to moisture conditions, Δ_{trc} correlations with humidity parameters are generally assumed to derive from CO_2-supply-side effects on DR discrimination (Gagen *et al*., 2022). By contrast, CO_2 assimilation responds to temperature and solar radiation, and corresponding Δ_{trc} correlations are generally assumed to derive from CO_2-demand-side effects on DR discrimination (Gagen *et al*., 2022). Moreover, there is a mechanistic relationship between DR discrimination and *iWUE* (Farquhar *et al*., 1982; Farquhar & Richards, 1984) which forms the basis of *iWUE* reconstructions from Δ_{trc} (Cernusak & Ubierna, 2022; Saurer & Voelker, 2022). *Nota bene*, all current Δ_{trc} interpretations assume DR discrimination governs Δ_{trc} variation (Gagen *et al*., 2022). Discrimination downstream of rubisco, denoted post-rubisco (PR) discrimination (Wieloch *et al*., 2018), is considered constant for any given species (Gessler *et al*., 2014; Cernusak & Ubierna, 2022).

Recently, nuclear magnetic resonance spectroscopy was used (for the first time in dendrochronology) to measure intramolecular ^{13}C discrimination, Δ_i', in glucose extracted across a series of tree rings from *Pinus nigra* Arnold (*i* denotes glucose carbon position C-1 to C-6; Supporting Information Notes S1) (Wieloch *et al*., 2018). Data of Δ_1', Δ_2', and Δ_3' pertaining to 1961–1980 (early period) and 1983–1995 (late period) were analysed separately as these series exhibit a change point in 1980 (Wieloch *et al*., 2025, pp. 1000–1017, in this issue of *New Phytologist*). Proposedly, the trees had access to groundwater during the early but not the late period (Wieloch *et al*., 2022a) causing metabolism affecting Δ_1' to Δ_3' to move from a homeostatic to a climate-responsive state (Wieloch *et al*., 2025). By contrast, no

---

This Viewpoint is based on findings by Wieloch *et al*. (2025), **245**: 1000–1017.

change point was detected in Δ_4', Δ_5', and Δ_6'. Based (*inter alia*) on multiple regression modelling, the dataset contains several ^{13}C signals (Tables 1, S1; Fig. S1). First, vapour pressure deficit (*VPD*) affects both Δ_1' and Δ_3' during the late period (Wieloch *et al.*, 2025). This relationship is thought to derive from DR discrimination. Additional leaf-level ^{13}C discrimination by phosphoglucose isomerase and/or glucose-6-phosphate dehydrogenase is thought to account for the stronger effect of *VPD* on Δ_1' compared to Δ_3'. Second, during the late period, Δ_1' and Δ_2' are related to ε_{met} denoting hydrogen isotope fractionation by metabolic processes at glucose H^1 and H^2, and ε_{met} can be substituted by precipitation (*PRE*) without losing much of the models' explanatory power (Wieloch *et al.*, 2022a, 2025). These relationships are thought to derive from ^{13}C discrimination by phosphoglucose isomerase and glucose-6-phosphate dehydrogenase in tree stems (Wieloch *et al.*, 2025). Note, the described Δ_1' to Δ_3' models do not work for the early period (Wieloch *et al.*, 2025). Third, global radiation (*RAD*) and temperature (*TMP*) affect Δ_4' to Δ_6' over the entire study period (Wieloch *et al.*, 2025). These relationships are thought to derive from leaf-level ^{13}C discrimination by glyceraldehyde-3-phosphate dehydrogenases affecting Δ_4' and enzymes modifying the carbon–carbon double bond of phospho*enol*pyruvate affecting Δ_5' and Δ_6' (Wieloch *et al.*, 2021, 2022b).

Here, the relative contributions of these intramolecular ^{13}C signals to whole-glucose ^{13}C discrimination (Δ_{glu}) were estimated by variance component analysis (Notes S2). As glucose extracted from tree rings largely derives from cellulose, the results can be expected to also apply to tree-ring cellulose (Δ_{trc}). They are used for a critical assessment of the classical concepts and practices of carbon-isotope dendrochronology. Subsequently, the potential value of intramolecular ^{13}C analysis for constraining impacts of tropospheric ozone on forest metabolism and productivity is discussed. Lastly, it is tested whether intramolecular ^{13}C signals can also be extracted from whole-molecule (Δ_{glu}) data.

Components of Δ_{glu} variation and implications for reconstructions of leaf intrinsic water-use efficiency

Leaf *iWUE* is regarded as an important functional property of plant ecosystems and a key determinant in the response of biogeochemical cycles to climate change (Beer *et al.*, 2009). Retrospective assessment of *iWUE* relies on Δ_{trc} analysis, which, in turn, relies on the assumption that DR discrimination governs Δ_{trc} variability (Ma *et al.*, 2021; Cernusak & Ubierna, 2022; Saurer & Voelker, 2022). Here, this assumption is critically examined.

(**1**) Fig. 1(a) shows percent contributions of intramolecular isotope signals found by modelling and model residuals to Δ_{glu} variation for the more dynamic late period (Δ_{glu} variance = 1.47‰) (Wieloch *et al.*, 2025). Leaf ^{13}C discrimination accounts for *c.* 43.5% of the total Δ_{glu} variance while stem ^{13}C discrimination (related to ε_{met}) accounts for *c.* 19.5%. The rest is residual variance (Notes S3). PR discrimination at the leaf- and stem-level (*c.* 25.9% and 19.5%, respectively) each exceed the contribution of DR discrimination (*c.* 8.8% × 2 = 17.6%).

(**2**) Similarly, Fig. 1(b) shows percent contributions of intramolecular isotope signals found by modelling and model residuals to Δ_{glu} variation for the less dynamic early period (Δ_{glu} variance = 0.36‰). Evidently, the contribution of Δ_1' to Δ_{glu} is negligible. Moreover, measurement error can account for the entire variation in Δ_2' (Notes S3). Hence, Δ_1' and Δ_2' are not considered further. However, *c.* 50% of the total Δ_3' variance may be systematic unmodelled variance (Notes S3). If we assume this variation results from DR discrimination, then DR discrimination accounts for *c.* 7.5% of the total Δ_{glu} variance (*c.* 0.5 × 15%) while PR discrimination accounts for *c.* 43.6%.

Table 1 Isotope-environment signals in Δ_i' and their proposed enzymatic origins (underlying Δ_i' models shown in Supporting Information Table S1; signal origins shown in Fig. S1).

			Proposed origin of introduction		
Covariate	Relationship	Period	Tissue	Enzyme	Discrimination type
$\Delta_1' \sim \varepsilon_{met}$[a]	Negative	83–95	Stem	PGI, G6PD	PR
$\Delta_1' \sim VPD$	Negative	83–95	Leaf	Rubisco,[b] PGI, G6PD	DR and PR
$\Delta_2' \sim \varepsilon_{met}$[a]	Negative	83–95	Stem	PGI	PR
$\Delta_3' \sim VPD$	Negative	83–95	Leaf	Rubisco[b]	DR
$\Delta_4' \sim RAD$	Negative	64–95	Leaf	p-GAPDH, np-GAPDH	PR
$\Delta_4' \sim TMP$	Positive	64–95	Leaf		
$\Delta_{5\text{-}6}' \sim RAD$	Negative	64–95	Leaf	PEPC, PK, DAHPS, Enolase	PR
$\Delta_{5\text{-}6}' \sim TMP$	Positive	64–95	Leaf		

ε_{met} denotes hydrogen isotope fractionation by metabolic processes at glucose H^1 and H^2. Δ_i' and $\Delta_{5\text{–}6}'$ denote ^{13}C discrimination at glucose carbon position, *i*, and the arithmetic average of Δ_5' and Δ_6', respectively. DR and PR refer to diffusion-rubisco and post-rubisco discrimination, respectively. Glucose was extracted across an annually resolved tree-ring series of *Pinus nigra* from the Vienna Basin. Climate data series: *RAD*, April–September global radiation (data available from 1964); *TMP*, March–October air temperature; *VPD*, March–November air vapour pressure deficit. Enzymes: DAHPS, 3-Deoxy-D-*arabino*-heptulosonate-7-phosphate synthase; G6PD, glucose-6-phosphate dehydrogenase; np- and p-GAPDH, nonphosphorylating and phosphorylating glyceraldehyde-3-phosphate dehydrogenase; PEPC, phospho*enol*pyruvate carboxylase; PGI, phosphoglucose isomerase; PK, pyruvate kinase.

[a] Replacing ε_{met} by March–July precipitation results in models with only slightly reduced explanatory power.

[b] ^{13}C discrimination during CO$_2$ diffusion and assimilation by rubisco is introduced into carbon metabolism at rubisco.

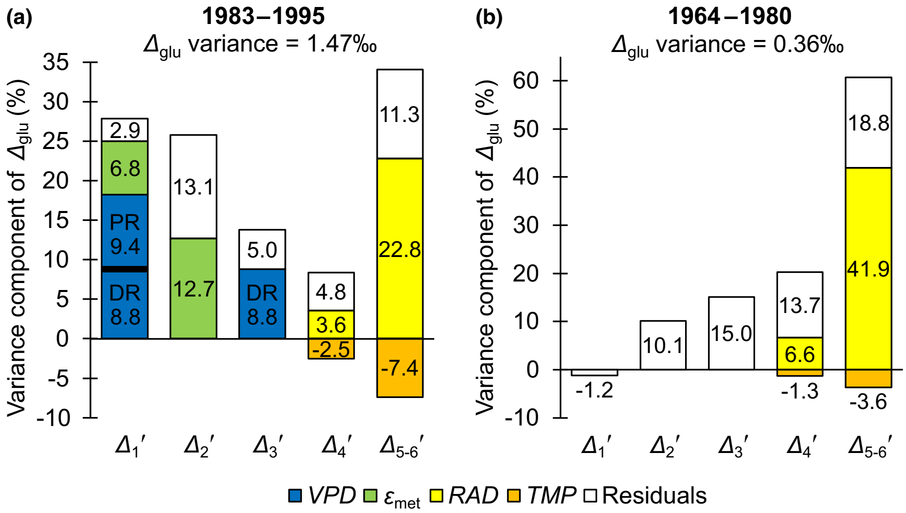

Fig. 1 Percent contributions of intramolecular carbon-isotope signals and model residuals to Δ_{glu} variation for the late (a) and early (b) period. According to current interpretation, the vapour pressure deficit (*VPD*) signal goes back to both diffusion-rubisco (DR) and post-rubisco (PR) discrimination (blue bars). All other signals go back to PR discrimination (green, yellow, and orange bars). Model residuals are shown as white bars. ε_{met} denotes hydrogen isotope fractionation by metabolic processes at glucose H^1 and H^2. Δ_i', $\Delta_{5\text{–}6}'$, and Δ_{glu} denote ^{13}C discrimination at glucose carbon position, *i*, and arithmetic averages of Δ_5' and Δ_6' and the whole molecule, respectively. *RAD* and *TMP* denote April–September global radiation and March–October air temperature, respectively. Glucose was extracted across an annually resolved tree-ring series of *Pinus nigra* from the Vienna Basin.

Hence, during both periods, DR discrimination is a comparably small contribution to total Δ_{glu} variation, which argues against using Δ_{trc} for reconstructions of interannual *iWUE* variation. As the *iWUE* signal is better resolved at the intramolecular level, Δ_i' analysis is expected to yield better estimates of *iWUE*.

Physiological interpretation of climate signals in Δ_{trc}

Currently, all reported Δ_{trc}–climate relationships are interpreted with respect to DR discrimination (Battipaglia & Cherubini, 2022; Churakova *et al.*, 2022; Gagen *et al.*, 2022; van der Sleen *et al.*, 2022). Thus, consideration is given only to two initial steps in the biosynthesis of tree-ring cellulose whereas ^{13}C discrimination by the numerous reactions downstream of rubisco (PR discrimination) is assumed to be constant (Fig. S1). However, recent reports of multiple intramolecular isotope signals in tree-ring glucose (Table 1) call for a critical reassessment of this practice.

At the site discussed here, DR discrimination responds to *VPD* (for information about the site, see notes S1 in Wieloch *et al.*, 2025). However, while DR discrimination accounts for *c.* 17.6% of the total variation of Δ_{glu} during the late period, *VPD*-dependent PR discrimination accounts for an additional *c.* 9.4% (Fig. 1a). Hence, both DR and PR discrimination contribute to the *VPD* signal in Δ_{glu} and their combined contribution accounts for *c.* 27% of the total Δ_{glu} variance. Interestingly, simple linear regression between Δ_{glu} and *VPD* falsely suggests that *VPD* accounts for *c.* 54% of the total Δ_{glu} variance (Fig. S2). This twofold overestimation of the actual *VPD* signal likely results from intercorrelation of *VPD* with other climate parameters that also affect Δ_{glu}. For instance, *RAD* affects tree-ring glucose C-5 and C-6 (Fig. 1a), and there is significant intercorrelation between *RAD* and *VPD* ($r = 0.6$, $P < 0.05$, $n = 13$) which will result in overestimation of the *VPD* signal in *VPD*-Δ_{glu} simple linear regression.

More importantly, relationships of Δ_{glu} with *RAD* and *TMP* derive from leaf-level PR discrimination (Wieloch *et al.*, 2021, 2022b, 2025), and *RAD*-dependent PR discrimination alone exceeds the contribution of DR discrimination to Δ_{glu} variation (Fig. 1, early period, *c.* 48.5% vs *c.* 7.5%; late period, *c.* 26.4% vs *c.* 17.6%). Similarly, relationships of Δ_{glu} with ε_{met} and *PRE* derive from stem-level PR discrimination (Wieloch *et al.*, 2025), and ε_{met}-dependent PR discrimination contributes similarly to Δ_{glu} variation as DR discrimination (Fig. 1a; *c.* 19.5% and 17.6%, respectively).

Hence, *RAD*-, *TMP*-, *PRE*-, and a fraction of the *VPD*-dependent Δ_{glu} variation is not caused by DR discrimination and associated physiological processes. Instead, most of the climate information in Δ_{glu} derives from PR discrimination and associated physiological processes.

New information from old archives – the impact of tropospheric ozone on forest metabolism

As shown recently, tree-ring glucose carries numerous carbon (and hydrogen) isotope signals (Wieloch *et al.*, 2018, 2022a), and there is considerable interest as to their scientific value in plant ecophysiology and biogeochemistry. For instance, the *RAD*-dependent carbon-isotope signal at tree-ring glucose C-5 and C-6 (Table 1) is thought to originate from ozone-induced metabolic adjustments (Wieloch *et al.*, 2022b). *RAD* promotes the photochemical formation of tropospheric ozone (Ainsworth *et al.*, 2012) which causes downregulation of rubisco and upregulation of PEPC (Saurer *et al.*, 1995; Dizengremel, 2001). Additionally, 3-deoxy-D-*arabino*-heptulosonate-7-phosphate synthase is expressed (Janzik *et al.*, 2005; Betz *et al.*, 2009). These biochemical adjustments can be expected to result in increased relative carbon flux into mitochondrial metabolism and the shikimate pathway (Fig. S1; Dizengremel, 2001). Hence, the isotope signal at C-5 and C-6 can potentially be used to reconstruct tropospheric ozone concentration, and ozone effects on forest metabolism and productivity.

In 2100, ozone is predicted to cause forest productivity losses of 17% relative to preindustrial air, which would have severe adverse

Table 2 Multiple linear regression models of Δ_{glu} as function of $\varepsilon_{\mathrm{met}}$, *VPD*, *RAD*, and *TMP*.

$\Delta_{\mathrm{glu}} \sim \varepsilon_{\mathrm{met}} + VPD + RAD + TMP$, 1983–1995			
$R^2 = 0.86$, adj$R^2 = 0.79$, $P < 0.002$, $n = 13$			
	Estimate	±SE	*P*
Intercept	25.0	5.2	≤ 0.001
$\varepsilon_{\mathrm{met}}$	−0.0142	0.0042	≤ 0.01
VPD	−0.00753	0.00475	= 0.15
RAD	−0.00475	0.00142	≤ 0.01
TMP	0.686	0.411=	= 0.13
$\Delta_{\mathrm{glu}} \sim RAD + TMP$, 1964–1980			
$R^2 = 0.5$, adj$R^2 = 0.42$, $P = 0.015$, $n = 15$			
	Estimate	±SE	*P*
Intercept	21.2	3.8	≤ 0.0001
RAD	−0.00350	0.00102	≤ 0.005
TMP	0.242	0.269	= 0.39

Δ_{glu} and $\varepsilon_{\mathrm{met}}$ denote whole-molecule ^{13}C discrimination of glucose and average hydrogen isotope fractionation caused by metabolic processes at glucose H^1 and H^2, respectively. Glucose was extracted across an annually resolved tree-ring series of *Pinus nigra* from the Vienna Basin. Climate data series: *RAD*, April–September global radiation; *TMP*, March–October air temperature; *VPD*, March–November air vapour pressure deficit.

effects on global carbon cycling and climate change (Wittig *et al*., 2009). However, this estimate relies strongly on short-term experiments on tree seedlings and saplings and may therefore not apply to mature natural forests (Emberson, 2020). The tree-ring isotope signal at glucose C-5 and C-6, on the other hand, can potentially be used to constrain ozone effects on mature natural forests across space and time. Similarly, other intramolecular carbon and hydrogen isotope signals detected in tree-ring glucose may help to advance our knowledge about other aspects of forest metabolism (Wieloch *et al*., 2025).

Mining whole-molecule data for information seen at the intramolecular level

Over the past decades, dendrochronologists have collected a wealth of (whole-molecule) Δ_{trc} data covering various forest biomes world-wide (e.g. Battipaglia & Cherubini, 2022; Churakova *et al*., 2022; van der Sleen *et al*., 2022). These data (*per se*) contain the same valuable information as (intramolecular) Δ_i' data. However, since Δ_{trc} has sixfold lower resolution than Δ_i', clear-cut extraction of Δ_i'-environment signals from Δ_{trc} data may not be feasible.

To test this, Δ_{glu} data of both study periods were modelled as function of all covariates known to significantly affect Δ_i' (cf Tables 1, S1). It was found that, during the late period, Δ_{glu} is significantly related to $\varepsilon_{\mathrm{met}}$ and *RAD* (Table 2, $P \leq 0.01$, $n = 13$), and close to significantly related to *VPD* and *TMP* ($P \leq 0.15$). By increasing the number of observations, all relationships might become significant. Moreover, the slope estimates of the Δ_{glu} model are not significantly different from those of the Δ_i' models (Fig. S3). During the early period, Δ_{glu} is significantly related to *RAD* (Table 2, $P \leq 0.005$, $n = 15$) but not *TMP* ($P = 0.39$). Still, the slope estimates of the Δ_{glu} model are not significantly different from those of the Δ_i' model (Fig. S4). Lastly, the change point separating the two study periods is detectable at both the intramolecular ($\Delta_{1\text{–}3}'$) and whole-molecule (Δ_{glu}) level (Wieloch *et al*., 2025).

Taken together, in the present case, most of the isotope-environment signals evident in Δ_i' can also be extracted from Δ_{glu}. Hence, reanalyses of existing Δ_{trc} datasets based on recent insights into plant isotope fractionation may yield both more accurate estimates of ecophysiological properties linked to DR discrimination (such as *iWUE*) and novel information about ecophysiological properties linked to PR discrimination (such as metabolic responses to ozone). That said, in Δ_{trc} analysis, the intramolecular location of any isotope-environment signal will always remain unknown which adds a level of uncertainty regarding the signal's metabolic origin and process specificity.

Conclusions and outlook

The picture emerging here is inconsistent with the classical (DR discrimination-centred) concepts and practices of carbon-isotope dendrochronology. Evidently, processes downstream of rubisco in leaves and stems introduced most of the isotope signals and variation in the tree-ring series examined. Hence, most of the ecophysiological and climate information in this record relates to PR processes. This opens new and exciting research avenues. First, the isotope signal reflecting *iWUE* is better resolved at the intramolecular than at the whole-molecule level. Careful separation of this signal from other signals in Δ_i' or Δ_{trc} is expected to yield more accurate estimates of *iWUE*. Second, an isotope signal at tree-ring glucose C-5 and C-6 reports metabolic changes in response to tropospheric ozone. Ozone is known for its severe adverse effects on forest productivity, global carbon cycling, and climate change. Analysing the signal at C-5 and C-6 may help to constrain these effects in natural forest ecosystems. Third, Δ_i' analysis gives access to deconvoluted information about multiple climate parameters and is therefore expected to enable distinctly more comprehensive paleoclimate reconstructions than Δ_{trc} analysis, providing an improved baseline for climate predictions (Wieloch *et al*., 2025). Fourth, recent and future insights into plant ^{13}C discrimination from Δ_i' analysis may enable extraction of information about multiple ecophysiological processes from existing Δ_{trc} datasets.

Taken together, Δ_i' analysis has significant disruptive potentials regarding the scientific development of the field of carbon-isotope dendrochronology. Unfortunately, measuring Δ_i' by nuclear magnetic resonance spectroscopy is labour-intensive and requires technology and know-how inaccessible to most dendrochronological laboratories. However, protocols enabling Δ_i' measurements by Orbitrap mass spectrometry are currently under development and may soon make Δ_i' data broadly accessible (Dion-Kirschner *et al*., 2023; Neubauer *et al*., 2023; Gessler *et al*., 2024). Moving from whole-molecule to intramolecular tree-ring isotope analysis is comparable to using a more powerful microscope and promises novel information about metabolism and climate across space and time (Wieloch *et al*., 2018, 2021, 2022a,b, 2025; Gessler *et al*., 2024).

Acknowledgements

This work was carried out with funding from 'Formas – a Swedish Research Council for Sustainable Development' (2022-02833, grant recipient: TW). I am grateful to Preprints.org (MDPI AG, Basel, Switzerland) for publishing preprints of this paper (https://www.preprints.org/manuscript/202403.0014/v2).

Competing interests

None declared.

ORCID

Thomas Wieloch https://orcid.org/0000-0001-9162-2291

Data availability

The author declares that the data supporting the findings of this study are available within the paper (Fig. 1; Tables 1, 2) and its Supporting Information (Notes S3; Figs S2–S4; Table S1).

Thomas Wieloch

Department of Forest Genetics and Plant Physiology, Swedish University of Agricultural Sciences, Umeå Plant Science Centre, 90183, Umeå, Sweden;
Division of Geological and Planetary Sciences, California Institute of Technology, 91125 Pasadena, CA, USA
(email thomas.wieloch@slu.se)

References

Ainsworth EA, Yendrek CR, Sitch S, Collins WJ, Emberson LD. 2012. The effects of tropospheric ozone on net primary productivity and implications for climate change. *Annual Review of Plant Biology* **63**: 637–661.

Battipaglia G, Cherubini P. 2022. Stable isotopes in tree rings of Mediterranean forests. In: Siegwolf RTW, Brooks JR, Roden J, Saurer M, eds. *Stable isotopes in tree rings: inferring physiological, climatic and environmental responses*. Cham, Switzerland: Springer International, 605–629.

Beer C, Ciais P, Reichstein M, Baldocchi D, Law BE, Papale D, Soussana J-F, Ammann C, Buchmann N, Frank D *et al*. 2009. Temporal and among-site variability of inherent water use efficiency at the ecosystem level. *Global Biogeochemical Cycles* **23**: GB2018.

Betz GA, Gerstner E, Stich S, Winkler B, Welzl G, Kremmer E, Langebartels C, Heller W, Sandermann H, Ernst D. 2009. Ozone affects shikimate pathway genes and secondary metabolites in saplings of European beech (*Fagus sylvatica* L.) grown under greenhouse conditions. *Trees* **23**: 539–553.

Cernusak LA, Ubierna N. 2022. Carbon isotope effects in relation to CO_2 assimilation by tree canopies. In: Siegwolf RTW, Brooks JR, Roden J, Saurer M, eds. *Stable isotopes in tree rings: inferring physiological, climatic and environmental responses*. Cham, Switzerland: Springer International, 291–310.

Churakova OV, Porter TJ, Kirdyanov AV, Myglan VS, Fonti MV, Vaganov EA. 2022. Stable isotopes in tree rings of boreal forests. In: Siegwolf RTW, Brooks JR, Roden J, Saurer M, eds. *Stable isotopes in tree rings: inferring physiological, climatic and environmental responses*. Cham, Switzerland: Springer International, 581–603.

Craig H. 1953. The geochemistry of the stable carbon isotopes. *Geochimica et Cosmochimica Acta* **3**: 53–92.

Craig H. 1954. Carbon-13 variations in Sequoia rings and the atmosphere. *Science* **119**: 141–143.

Dion-Kirschner H, KongJohnson C, Sharp K, Dalleska NF, Eiler JM, Sessions AL. 2023. Position-specific carbon isotope analysis of tree ring cellulose via Orbitrap mass spectrometry. AGU fall meeting abstracts: H51H-07. [WWW document] URL https://agu.confex.com/agu/fm23/meetingapp.cgi/Paper/1409820.

Dizengremel P. 2001. Effects of ozone on the carbon metabolism of forest trees. *Plant Physiology and Biochemistry* **39**: 729–742.

Emberson L. 2020. Effects of ozone on agriculture, forests and grasslands. *Philosophical Transactions of the Royal Society A: Mathematical, Physical and Engineering Sciences* **378**: 20190327.

Evans JR, Farquhar GD, Sharkey TD, Berry JA. 1986. Carbon isotope discrimination measured concurrently with gas exchange to investigate CO_2 diffusion in leaves of higher plants. *Australian Journal of Plant Physiology* **13**: 281–292.

Farquhar GD, O'Leary MH, Berry JA. 1982. On the relationship between carbon isotope discrimination and the intercellular carbon dioxide concentration in leaves. *Australian Journal of Plant Physiology* **9**: 121–137.

Farquhar GD, Richards RA. 1984. Isotopic composition of plant carbon correlates with water-use efficiency of wheat genotypes. *Australian Journal of Plant Physiology* **11**: 539–552.

Gagen M, Battipaglia G, Daux V, Duffy J, Dorado-Liñán I, Hayles LA, Martínez-Sancho E, McCarroll D, Shestakova TA, Treydte K. 2022. Climate signals in stable isotope tree-ring records. In: Siegwolf RTW, Brooks JR, Roden J, Saurer M, eds. *Stable isotopes in tree rings: inferring physiological, climatic and environmental responses*. Cham, Switzerland: Springer International, 537–579.

Gessler A, Ferrio JP, Hommel R, Treydte K, Werner RA, Monson RK. 2014. Stable isotopes in tree rings: towards a mechanistic understanding of isotope fractionation and mixing processes from the leaves to the wood. *Tree Physiology* **34**: 796–818.

Gessler A, Wieloch T, Saurer M, Lehmann MM, Werner RA, Kammerer B. 2024. The marriage between stable isotope ecology and plant metabolomics – new perspectives for metabolic flux analysis and the interpretation of ecological archives. *New Phytologist* **244**: 21–31.

Helle G, Pauly M, Heinrich I, Schollän K, Balanzategui D, Schürheck L. 2022. Stable isotope signatures of wood, its constituents and methods of cellulose extraction. In: Siegwolf RTW, Brooks JR, Roden J, Saurer M, eds. *Stable isotopes in tree rings: inferring physiological, climatic and environmental responses*. Cham, Switzerland: Springer International, 135–190.

Janzik I, Preiskowski S, Kneifel H. 2005. Ozone has dramatic effects on the regulation of the prechorismate pathway in tobacco (*Nicotiana tabacum* L. cv. Bel W3). *Planta* **223**: 20–27.

Ma WT, Tcherkez G, Wang XM, Schäufele R, Schnyder H, Yang Y, Gong XY. 2021. Accounting for mesophyll conductance substantially improves ^{13}C-based estimates of intrinsic water-use efficiency. *New Phytologist* **229**: 1326–1338.

McCarroll D, Loader NJ. 2004. Stable isotopes in tree rings. *Quaternary Science Reviews* **23**: 771–801.

Neubauer C, Kantnerová K, Lamothe A, Savarino J, Hilkert A, Juchelka D, Hinrichs K-U, Elvert M, Heuer V, Elsner M *et al*. 2023. Discovering nature's fingerprints: isotope ratio analysis on bioanalytical mass spectrometers. *Journal of the American Society for Mass Spectrometry* **34**: 525–537.

Saurer M, Maurer S, Matyssek R, Landolt W, Günthardt-Goerg MS, Siegenthaler U. 1995. The influence of ozone and nutrition on $\delta^{13}C$ in *Betula pendula*. *Oecologia* **103**: 397–406.

Saurer M, Voelker S. 2022. Intrinsic water-use efficiency derived from stable carbon isotopes of tree-rings. In: Siegwolf RTW, Brooks JR, Roden J, Saurer M, eds. *Stable isotopes in tree rings: inferring physiological, climatic and environmental responses*. Cham, Switzerland: Springer International, 481–498.

van der Sleen P, Zuidema PA, Pons TL. 2022. Stable isotopes in tree rings of tropical forests. In: Siegwolf RTW, Brooks JR, Roden J, Saurer M, eds. *Stable isotopes in tree rings: inferring physiological, climatic and environmental responses*. Cham, Switzerland: Springer International, 631–649.

Voelker SL, Brooks JR, Meinzer FC, Anderson R, Bader MK-F, Battipaglia G, Becklin KM, Beerling D, Bert D, Betancourt JL *et al*. 2016. A dynamic leaf gas-exchange strategy is conserved in woody plants under changing ambient CO_2: evidence from carbon isotope discrimination in paleo and CO_2 enrichment studies. *Global Change Biology* **22**: 889–902.

Wieloch T, Ehlers I, Yu J, Frank D, Grabner M, Gessler A, Schleucher J. 2018. Intramolecular ^{13}C analysis of tree rings provides multiple plant ecophysiology signals covering decades. *Scientific Reports* **8**: 5048.

Wieloch T, Grabner M, Augusti A, Serk H, Ehlers I, Yu J, Schleucher J. 2022a. Metabolism is a major driver of hydrogen isotope fractionation recorded in tree-ring glucose of *Pinus nigra*. *New Phytologist* **234**: 449–461.

Wieloch T, Holloway-Phillips M, Yu J, Niittylä T. 2025. New insights into the mechanisms of plant isotope fractionation from combined analysis of intramolecular ^{13}C and deuterium abundances in *Pinus nigra* tree-ring glucose. *New Phytologist* **245**: 1000–1017.

Wieloch T, Sharkey TD, Werner RA, Schleucher J. 2022b. Intramolecular carbon isotope signals reflect metabolite allocation in plants. *Journal of Experimental Botany* **73**: 2558–2575.

Wieloch T, Werner RA, Schleucher J. 2021. Carbon flux around leaf-cytosolic glyceraldehyde-3-phosphate dehydrogenase introduces a ^{13}C signal in plant glucose. *Journal of Experimental Botany* **72**: 7136–7144.

Wittig VE, Ainsworth EA, Naidu SL, Karnosky DF, Long SP. 2009. Quantifying the impact of current and future tropospheric ozone on tree biomass, growth, physiology and biochemistry: a quantitative meta-analysis. *Global Change Biology* **15**: 396–424.

Supporting Information

Additional Supporting Information may be found online in the Supporting Information section at the end of the article.

Notes S1 Isotope data.

Notes S2 Variance component analysis.

Notes S3 Model residuals.

Fig. S1 Proposed metabolic origins of carbon-isotope signals in tree-ring glucose.

Fig. S2 Linear regression between whole-molecule ^{13}C discrimination of tree-ring glucose and March–November air vapour pressure deficit for the late period.

Fig. S3 Comparison of slope estimates from the whole-molecule vs intramolecular isotope-environment models for the late study period.

Fig. S4 Comparison of slope estimates from the whole-molecule vs intramolecular isotope-environment models for the early study period.

Table S1 Multiple linear regression models of $\Delta_i{}'$ as function of ε_{met}, March–November air vapour pressure deficit, March–July precipitation, April–September global radiation, and March–October air temperature.

Key words: carbon stable isotopes, dendrochronology, intramolecular isotope analysis, paleoclimate reconstruction, plant carbon fluxes, tree rings, water-use efficiency, whole-molecule isotope analysis.

Received, 1 July 2024; accepted, 22 October 2024.